

Structure and properties of *N*-heterocycle-containing benzotriazoles as UV absorbers



Zhihua Cui^{a,b}, Xin Li^b, Xidong Wang^b, Kemei Pei^{a,c,*}, Weiguo Chen^{a,b}

^aKey Laboratory of Advanced Textile Materials and Manufacturing Technology, Ministry of Education of China, Zhejiang Sci-Tech University, Hangzhou 310018, China

^bEngineering Research Center for Eco-Dyeing & Finishing of Textiles, Ministry of Education, Zhejiang Sci-Tech University, Hangzhou 310018, China

^cDepartment of Chemistry, Zhejiang Sci-Tech University, Hangzhou 310018, China

HIGHLIGHTS

- Two novel *N*-heterocycle-bearing UVAs were synthesized.
- The excellent absorption comes from S₀ → S₁ electronic transition band of the Enol forms.
- **CBHDCP** and **CBMPP** show much higher ϵ_{max} than commercial UVA Tinuvin 326.

ARTICLE INFO

Article history:

Received 29 July 2013

Received in revised form 20 September 2013

Accepted 23 September 2013

Available online 1 October 2013

Keywords:

Benzotriazole

UV absorber

UV-visible spectroscopy

Molecular orbital calculations

ABSTRACT

Two *N*-heterocycle-containing benzotriazole compounds (**CBHDCP**, **CBMPP**) were synthesized and their structures were confirmed by FT-IR, ¹H NMR, mass spectroscopy and elemental analysis. Their spectral properties compared with that of a common commercial benzotriazole UV absorber Tinuvin 326 in solvents were measured and analyzed using molecular orbital calculations. It was found that the experimentally obtained optical properties were in close agreement with the theoretically obtained results. Besides, **CBMPP** is much superior to **CBHDCP** acting as an effective UV absorber on polyethylene terephthalate fabric due to its combinative higher exhaustion and higher molar extinction coefficient. The exhaustion difference on polyethylene terephthalate fabric among *N*-heterocycle-containing benzotriazoles (**CBHDCP**, **CBMPP**) and Tinuvin 326 were then measured and explained by the solubility parameter theory. The results agreed with the rule that compounds with higher exhaustion on fiber have solubility parameter much closer to that of fiber polymer.

© 2013 Elsevier B.V. All rights reserved.

1. Introduction

It is widely recognized that ultraviolet rays (UVR) in sunlight (wavelengths between 280 nm and 400 nm) is an important factor causing skin aging, eye disease [1] and photodegradation to some organic substances such as polymers and colorants [2,3]. With the ozone depletion in recent years, much more UVR has been progressively reached the earth surface [4] and causes severe photo-induced loss to organic materials. In order to protect against the damaging effects of UVR on organic materials, addition of UV absorber (UVA) is an effective and convenient solution in practice [5,6].

An ideal UVA must have the key property: highly efficient absorption between 280 and 400 nm coupled with high optical transparency in the visible range. 2-(2-Hydroxyphenyl)-benzotriazole derivatives are one sort of efficient UVA absorbing in the

wavelength region of 300–360 nm and hardly absorbing visible light. The photostabilization mechanism of these type of compounds is based on the formation of intramolecular hydrogen bonds (IMHB) between the *o*-hydroxyl group of the phenyl ring and the nitrogen atom of the benzotriazole moiety and the excited state intramolecular proton transfer (ESIPT) mechanism by O···H···N tunneling (Fig. 1) [7].

Since the discovery of 2-(2-hydroxyphenyl)-benzotriazole as a UVA chromophore, most efforts have been focused on the effect of substituent variation in benzotriazole chromophore [8,9] than chromophore variation itself. In view of the introduction of heterocycle to chromophore bringing lots of interesting properties, in this work, heterocycle moiety was introduced to benzotriazole chromophore and two novel *N*-heterocycle-containing benzotriazole compounds (**CBHDCP**, **CBMPP**) were designed. The calculation results predicted they had much higher molar extinction coefficients than that of Tinuvin 326, a common commercial benzotriazole UVA. Then **CBHDCP** and **CBMPP** were synthesized from reactant 4-chloro-2-nitroaniline via diazotization, azo coupling, reductive cyclization, acidification (Scheme 1) and characterized by FT-IR,

* Corresponding author at: Key Laboratory of Advanced Textile Materials and Manufacturing Technology, Ministry of Education of China, Zhejiang Sci-Tech University, Hangzhou 310018, China. Tel.: +86 571 86843627.

E-mail address: xiaopei027@sina.com (K. Pei).

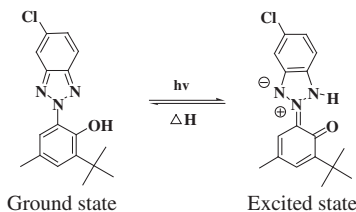


Fig. 1. The excited state intramolecular proton transfer (ESIPT) mechanism of Tinuvin 326.

^1H NMR, mass spectroscopy as well as elemental analysis. Quantum chemistry calculations were carried out to investigate the stable structure and UV electronic absorption bands of **CBHDCP**, **CBMPP** and Tinuvin 326.

The prepared **CBHDCP** and **CBMPP** were then applied to polyethylene terephthalate (PET) fabric by exhaustion dyeing method due to their good hydrophobicity similar to the disperse dyes, which had affinity to PET fiber and absorbed on it. The dyeing exhaustion of **CBHDCP**, **CBMPP** and Tinuvin 326 on PET fabric have also been calculated by experimental, and then explained by the solubility parameter theory.

2. Theoretical methodology

Density functional theory (DFT) and time dependent (TD) calculations were done to determine the optimized geometry and UV absorption spectra. Therefore, in this work, by allowing the relaxation of all the parameters, calculation has been found to converge to a optimized geometry at B3LYP/6-31G(d) level, as revealed by the absence of imaginary values in the calculated wavenumbers of all the vibrational modes, while the electronic transition energies and electronic transition orbital were calculated by B3LYP-TD/6-31G(d) method. Cluster model and the self-consistent isodensity polarizable continuum model (SCI-PCM) were used to explain the UV absorption spectra of **CBHDCP** in ethanol solution. All the quantum mechanical calculations in this paper were carried out in the Gaussian09 program [10].

The solubility parameters of UVA were estimated using the group contribution method according to Eq. (1). For calculating the solubility parameters of the UVA molecules, the values of cohesive energy (E_{cohi}) and molar volume (V_{mi}) for each functional group at 25 °C were obtained from Fedor's data [11].

$$\delta = \left(\frac{\sum E_{cohi}}{\sum V_{mi}} \right)^{1/2} \quad (1)$$

where δ is the solubility parameter of a molecule; E_{cohi} is the cohesive energy for i functional group on the molecule, and V_{mi} is its molar volume.

3. Experimental

3.1. Materials, equipment and analysis

The reagents, 4-chloro-2-nitroaniline, sodium nitrite, *N*-methyl-3-cyano-6-hydroxy-4-methyl-2-pyridone and 1-phenyl-3-methyl-5-pyrazolone, concentrated hydrochloric acid, thiourea dioxide, sodium carbonate, sodium hydroxide and the dispersant sodium methylenedipthalene disulphonate (NNO) were bought from Aladdin Reagent Co. Ltd (Shanghai, China). Tinuvin 326 was bought from Shinyang Chemical Co. Ltd (Hangzhou, China).

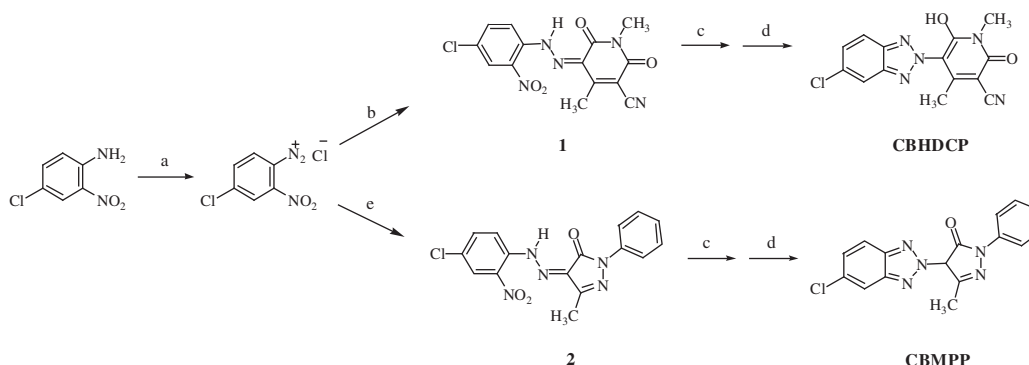
Proton nuclear magnetic resonance (^1H NMR) spectra were recorded on a Varian Inova 400 NMR spectrometer (Varian, USA) with tetramethylsilane (TMS) as internal standard in $\text{DMSO-}d_6$. Infrared spectra were measured with a Fourier Transform–infrared (FTIR)–430 spectrophotometer (Jasco Co., Japan). Mass spectra (MS) were recorded on an HP1100 HPLC/MS system (HP Co., USA) using electrospray ionisation (ESI) mode. Ultraviolet–visible (UV–vis) absorption spectra were recorded on a Lambda 900 UV–vis spectrophotometer (Perkin–Elmer Co., USA).

3.2. Synthesis of **CBHDCP** and **CBMPP**

The synthesis processes of benzotriazole **CBHDCP** and **CBMPP** are shown in Scheme 1. Firstly, compound **1** and **2** were synthesized from 4-chloro-2-nitroaniline diazonium salts with *N*-methyl-3-cyano-6-hydroxy-4-methyl-2-pyridone and 1-phenyl-3-methyl-5-pyrazolone using classical reaction for the synthesis of the azocompounds [12]. Subsequently, compound **1** (0.05 mol) was dissolved in aqueous solution containing NaOH (0.55 mol) and water (300 mL). The solution was heated and kept the temperature at about 83 °C, and thiourea dioxide (0.25 mol) was added in four times within 2 h. After a total reaction time of 3 h, the solution was poured in ice water and acidified to pH 2.0 with concentrated hydrochloric acid, and then the product **CBHDCP** was filtered and dried in vacuum. **CBMPP** was also synthesized using the same process described above where compound **1** was replaced by compound **2**. The crude products of **CBHDCP** and **CBMPP** were purified by recrystallisation with ethanol.

5-(5-Chloro-2-benzotriazolyl)-6-hydroxy-1,4-dimethyl-3-carbonitrile-2-pyridone (**CBHDCP**): Yield: 86%. FTIR (ATR/ cm^{-1}): 3346 (OH), 2206 (CN), 1643 (C=O), 1106 (C–Cl). ^1H NMR (400 MHz, $\text{DMSO-}d_6$): δ 8.11 (s, 1H, Ar–H), 8.02 (d, 1H, Ar–H), 7.46 (d, 1H, Ar–H), 3.12 (s, 3H, N–CH₃), 1.68 (s, 3H, CH₃). MS (ESI, negative): m/z 314.4 [(M–H)[–], 100%], 316.4 [(M–H+2)[–], 36%]. Element analysis: Found (%): C, 53.21, H, 3.24, N, 22.23; Calcd. (%): C, 53.26; H, 3.19; N, 22.18.

4-(5-Chloro-2-benzotriazolyl)-5-methyl-2-phenyl-3-pyrazolone (**CBMPP**): Yield: 88%. FTIR (ATR/ cm^{-1}): 2818 (CH₃), 1631 (C=O),



Scheme 1. Synthetic routes of *N*-heterocycle-containing benzotriazole compounds. Reagents and conditions: (a) NaNO_2/HCl ; (b) *N*-methyl-3-cyano-6-hydroxy-4-methyl-2-pyridone, Na_2CO_3 , 0–5 °C; (c) thiourea dioxide, NaOH, 83 °C, 3 h; (d) HCl; (e) 1-phenyl-3-methyl-5-pyrazolone, 0–5 °C.

1049 (C–Cl). $^1\text{H NMR}$ (400 MHz, $\text{DMSO-}d_6$): δ 8.08 (s, 1H, Ar–H), 7.99 (d, 1H, Ar–H), 7.94 (d, 2H, Ar–H), 7.43 (d, 1H, Ar–H), 7.40 (d, 2H, Ar–H), 7.18–7.16 (m, 1H, Ar–H), 2.25 (s, 3H, CH_3). MS (ESI, positive): m/z [348.2($\text{M}+\text{Na}$) $^+$, 100%], [350.2($\text{M}+\text{Na}+2$) $^+$, 39%]. Element analysis: Found (%): C, 59.06, H, 3.67, N, 21.44; Calcd. (%): C, 58.99, H, 3.71, N, 21.50.

3.3. Dyeing to PET fabric

Benzotriazole **CBHDCP**, **CBMPP** and Tinuvin 326 had been milled in the presence of a dispersant NNO (1:1 w/w) with glass beads (1 mm in diameter) for 4 h to form their aqueous suspension, respectively. Then the aqueous suspensions were applied to PET fabrics by an exhaustion dyeing at conditions of liquor-to-fabric of 40:1, concentration of 0.5–2.0% on weight of fiber (owf) and dyebath pH 5.0. Dyeing was started at room temperature and increased to 130 °C at a rate of 2 °C min^{-1} , and held for 1 h before cooling to room temperature. Then the fabrics were taken out, rinsed with water and finally air-dried.

3.4. Measurement of exhaustion

The UVA in the residual dye bath and staining inside the dyeing pot were rinsed with acetone and dissolved into 50/50 acetone/water. The optical absorbance of the solutions was determined according to Lambert–Beer's law at the maximum absorption wavelength of each dye by UV–vis spectrophotometer. Subsequently, the exhaustion was calculated using Eq. (2).

$$\text{Exhaustion (\%)} = [(A_1 - A_2)/A_1] \times 100\% \quad (2)$$

where A_1 and A_2 are the absorbance of the dye bath dissolved into 50/50 acetone/water before and after dyeing.

4. Results and discussion

4.1. Synthesis and characteristic

Both benzotriazole **CBHDCP** and **CBMPP** may exist in different tautomeric forms (Enol form and Keto form) under unexcited states (Fig. 2). The infrared spectrum of benzotriazole **CBHDCP** detected in solid state shows one broad hydroxyl band at about 3346 cm^{-1} , which is assigned to the Enol form (Enol (1) or Enol

(2)). The infrared spectrum of benzotriazole **CBMPP** detected in solid state shows one intense carbonyl band at about 1631 cm^{-1} , which is assigned to the Keto form. Both of them can mainly exist as or convert to Enol form firstly and absorb UV light by ESIPT mechanism similar to other 2-(2-Hydroxyphenyl)-benzotriazole derivatives (Fig. 1). In the $^1\text{H NMR}$ spectra of benzotriazole **CBHDCP** and **CBMPP**, the signal corresponding to CH proton resonance of the Keto form does not appear. It indicates benzotriazole **CBHDCP** and **CBMPP** mainly exist as Enol form in $\text{DMSO-}d_6$ solution despite their active hydrogen signal in OH often disappear due to hydrogen exchange with $\text{DMSO-}d_6$.

4.2. UV–vis absorption spectrum

The UV–vis spectra of the benzotriazole derivatives **CBHDCP**, **CBMPP** and Tinuvin 326 measured in ethanol and chloroform according to their solubility are shown in Fig. 3(a and b), respectively. As shown in Fig. 3, the maximum absorption wavelength (λ_{max}) of benzotriazole **CBHDCP** and **CBMPP** are at 327 nm in ethanol and 340 nm in chloroform, respectively. And only one sharp peak appears in the range of 280–400 nm, which has great difference with Tinuvin 326 exhibiting two peaks at about 310 nm and 350 nm. The molar extinction coefficient (ϵ_{max}) of benzotriazole **CBHDCP** (27,000 $\text{L mol}^{-1} \text{cm}^{-1}$ at 327 nm in ethanol) and benzotriazole **CBMPP** (28,500 $\text{L mol}^{-1} \text{cm}^{-1}$ at 340 nm in chloroform) is much larger than that of Tinuvin 326 (18,900 $\text{L mol}^{-1} \text{cm}^{-1}$ at 351 nm in ethanol, 16,300 $\text{L mol}^{-1} \text{cm}^{-1}$ at 353 nm in chloroform).

Quantum chemistry method TD DFT has been used to simulate the UV–vis absorption spectra successfully [13–15]. In this paper, the UV absorption data of two synthesized *N*-heterocycle-containing benzotriazole UVAs (**CBHDCP** and **CBMPP**) were analyzed by quantum chemistry calculations. The TD calculation results about electronic absorption band, oscillator strength, molar extinction coefficient and maximum absorption wavelength above 250 nm wavelength range are listed in Table 1. As shown in Table 1, based on gas monomolecular model, the two UVAs display high calculated maximum molar extinction coefficient 21,000 $\text{L mol}^{-1} \text{cm}^{-1}$ (**CBHDCP**) and 27,000 $\text{L mol}^{-1} \text{cm}^{-1}$ (**CBMPP**) as well as strong absorption range in 280–380 nm UV region, matching ideal UV absorption properties.

The agreement between the simulated $S_0 \rightarrow S_1$ electronic transition band of **CBHDCP** and **CBMPP** in their Enol forms and the

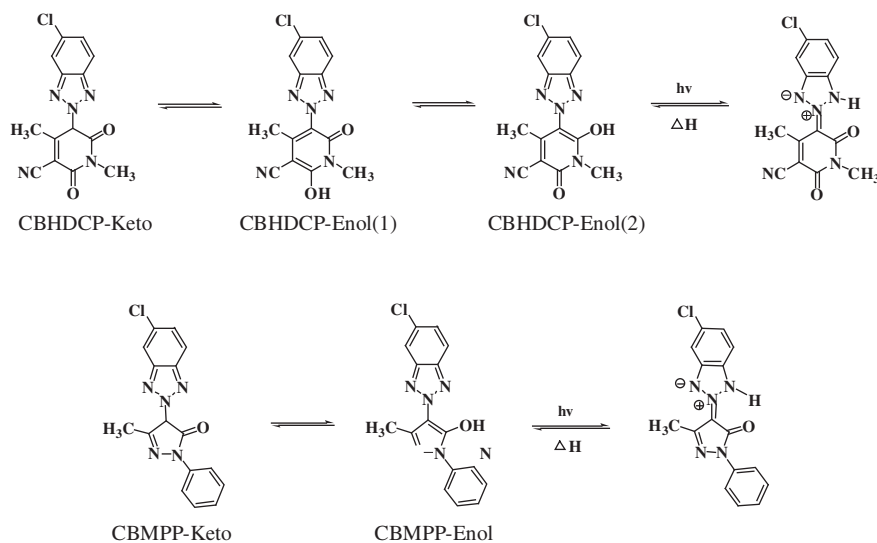


Fig. 2. The tautomerism between keto and Enol forms of **CBHDCP**, **CBMPP** and their UV absorbing mechanism.

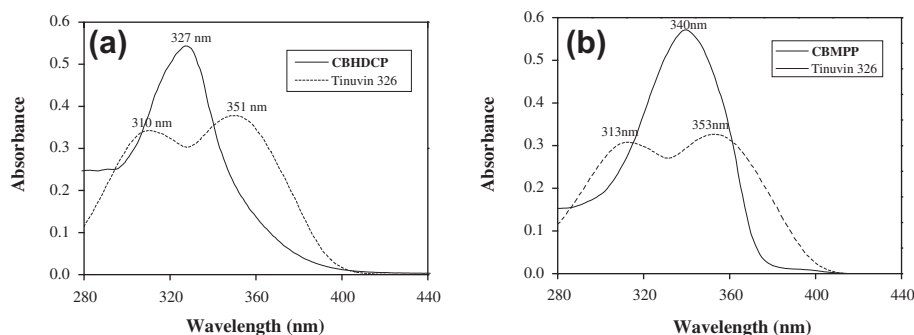


Fig. 3. UV-vis absorption spectra of benzotriazole **CBHDCP**, **CBMPP** and Tinuvin 326. (a) in ethanol (2×10^{-5} mol/L); (b) in chloroform (2×10^{-5} mol/L).

Table 1

TD calculation results about electronic absorption band, oscillator strength, molar extinction coefficient and maximum absorption wavelength above 250 nm wavelength range.

| Transition state | Oscillator strength (f) | Molar extinction coefficient ($L \text{ mol}^{-1} \text{ cm}^{-1}$) | | Maximum absorption wavelength (nm) | |
|-----------------------|-------------------------|---|---------------------------------------|------------------------------------|--------------------------------|
| | | Calcd. | Expt. | Calcd. | Expt. |
| Tinuvin 326 | | | | | |
| S0 → S1 | 0.2574 | 14,000 | 18,900 (ethanol), 16,300 (chloroform) | 376 | 353 (ethanol) 355 (chloroform) |
| S0 → S2 | 0.4135 | | | 315 | 310 (ethanol) 313 (chloroform) |
| S0 → S3 | 0.0595 | | | 291 | |
| S0 → S4 | 0.0190 | | | 251 | |
| CBHDCP-Enol(1) | | | | | |
| S0 → S1 | 0.1781 | 12,000 | | 311 | |
| S0 → S2 | 0.1016 | | | 302 | |
| S0 → S3 | 0.0405 | | | 280 | |
| S0 → S4 | 0.0755 | | | 274 | |
| S0 → S5 | 0.0220 | | | 267 | |
| S0 → S6 | 0.0105 | | | 262 | |
| S0 → S7 | 0.0294 | | | 253 | |
| CBHDCP-Enol(2) | | | | | |
| S0 → S1 | 0.5098 (0.6291) | 21,000 (25,500) | 27,000 (ethanol) | 373 (349) | 327 (ethanol) |
| S0 → S2 | 0.1494 (0.0918) | | | 313 (297) | |
| S0 → S3 | 0.0471 (0.0455) | | | 296 (280) | |
| S0 → S4 | 0.0002 (0) | | | 280 (274) | |
| S0 → S5 | 0.1452 (0.0109) | | | 267 (261) | |
| S0 → S6 | 0.0062 (0.0901) | | | 260 (261) | |
| S0 → S7 | 0.0002 (0.0002) | | | 256 (259) | |
| CBHDCP-Keto | | | | | |
| S0 → S1 | 0.0002 | | | 348 | |
| S0 → S2 | 0.0130 | | | 308 | |
| S0 → S3 | 0.0078 | | | 302 | |
| S0 → S4 | 0.1098 | | | 282 | |
| S0 → S5 | 0.0260 | | | 265 | |
| S0 → S6 | 0.0128 | | | 264 | |
| S0 → S7 | 0.1956 | | | 262 | |
| CBMPP-Enol | | | | | |
| S0 → S1 | 0.5738 | 27,000 | 28,500 (chloroform) | 342 | 340 (chloroform) |
| S0 → S2 | 0.1791 | | | 328 | |
| S0 → S3 | 0.0551 | | | 286 | |
| S0 → S4 | 0.0034 | | | 274 | |
| S0 → S5 | 0.1282 | | | 252 | |
| CBMPP-Keto | | | | | |
| S0 → S1 | 0.0120 | | | 339 | |
| S0 → S2 | 0.0217 | | | 318 | |
| S0 → S3 | 0.0016 | | | 285 | |
| S0 → S4 | 0.1460 | | | 284 | |
| S0 → S5 | 0.0014 | | | 274 | |
| S0 → S6 | 0.0109 | | | 270 | |
| S0 → S7 | 0.2845 | | | 268 | |
| S0 → S8 | 0.0002 | | | 265 | |

Note: The data in parentheses are obtained based on cluster model and SCI-PCM solution model, and other calculation results are based on gas monomolecular model.

experimental spectra (**CBHDCP**: $27,000 L \text{ mol}^{-1} \text{ cm}^{-1}$ at 327 nm in ethanol, **CBMPP**: $28,500 L \text{ mol}^{-1} \text{ cm}^{-1}$ at 340 nm in chloroform) is excellent, as shown in Table 1. Therefore both **CBHDCP** in ethanol and **CBMPP** in chloroform are Enol form, which agree with the ^1H

NMR characterization results. The optimized structures of **CBHDCP** in ethanol and **CBMPP** in chloroform in Enol form are shown in Fig. 4. Fig. 4 clearly shows that the skeleton cyclic structure of **CBHDCP-Enol(2)** are in different planes, but the skeleton structure

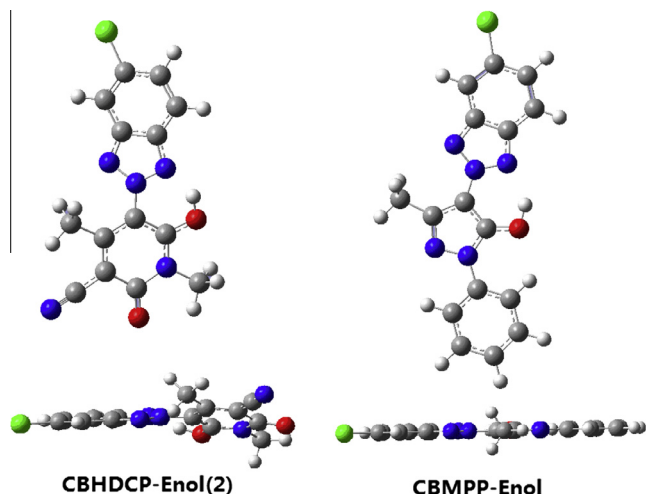


Fig. 4. The optimized structures of **CBHDCP-Enol(2)** and **CBMPP-Enol** at B3LYP-TD/6-31G(d) theoretical level.

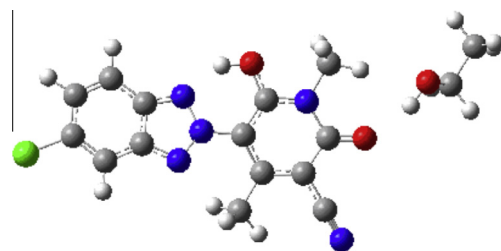


Fig. 5. Cluster model of **CBHDCP-Enol**– $\text{CH}_3\text{CH}_2\text{OH}$.

of **CBMPP-Enol** is planar with C_s symmetry. As for **CBHDCP-Enol(2)** with cyclic ketone structure, the carbonyl group interaction with protic solvents such as ethanol by hydrogen bond influence its UV absorption spectrum significantly. Herein, the hydrogen bond interaction and solvent polar effect should be considered for calculating UV–vis absorption spectrum of **CBHDCP** in ethanol solution.

Subsequently, cluster model (Fig. 5) for hydrogen bond interaction and self-consistent isodensity polarizable continuum model (SCI-PCM) for solvent polar effect have been selected, as Table 1 listed. As the data in parentheses of Table 1 shown, the model which considers the hydrogen bond interaction and solvent polar effect can give more anastomotic results on molar extinction coefficient and maximum absorption wavelength in comparison with the experimental results.

4.3. Exhaustion and UPF

The exhaustion and UV protection data of **CBHDCP**, **CBMPP** and Tinuvin 326 on PET fabric were listed in Table 2. It was clear that all

Table 2
Exhaustion and UPF data recorded on dyed PET fabric.

| Owf/% | Benzotriazole CBHDCP | | Benzotriazole CBMPP | | Tinuvin 326 | |
|-------|-----------------------------|-----|----------------------------|-----|--------------|-----|
| | Exhaustion/% | UPF | Exhaustion/% | UPF | Exhaustion/% | UPF |
| 0.5 | 10.9 | 62 | 63.2 | 183 | 97.2 | 294 |
| 1.0 | 5.4 | 67 | 56.9 | 226 | 93.5 | 385 |
| 2.0 | 3.9 | 75 | 51.0 | 380 | 75.6 | 440 |

The UPF of blank PET fabric is 37.

Table 3

The solubility parameters of **CBHDCP**, **CBMPP** and Tinuvin 326 estimated using the group contribution method.

| Data | CBHDCP-Enol | CBMPP-Keto | Tinuvin 326 | PET |
|----------------------|--------------------|-------------------|-------------|------|
| E_{coh} | 173768 | 154165 | 147866 | – |
| V_m | 137 | 156.2 | 175 | – |
| Solubility parameter | 35.6 | 31.4 | 29.1 | 23.5 |

The solubility parameter of PET was calculated based on E_{coh} and V_m values from Hoy.

dyed fabric samples with UVA provided effective protection against UVR. The application of benzotriazole **CBHDCP** at 0.5% owf increased the ultraviolet protection factor (UPF) to 62 (the UPF of blank PET fabric is only 37). However, with the amount increase of benzotriazole **CBHDCP** to 1.0% owf and even 2.0% owf, no obvious UPF increase for PET fabric was found which may be induced by their poor exhaustion (less than 11%). On the contrary, benzotriazole **CBMPP** has better exhaustion on PET fabric (more than 50%) than **CBHDCP**. The application of benzotriazole **CBMPP** at 0.5% owf sharply increased the UPF over 180. The UPF of PET fabric reached 380 with the application of benzotriazole **CBMPP** at 2.0% owf, which is close to the ultraviolet protection effect of Tinuvin 326 on PET at 1.0% owf even though the exhaustion of **CBMPP** (51%) is much lower than that of Tinuvin 326 (93.5%). The higher UPF of the dyed PET fabric means benzotriazole **CBMPP** is much superior to benzotriazole **CBHDCP** and acts as an effective UVA due to its combinative higher exhaustion and higher molar extinction coefficient compared with benzotriazole **CBHDCP**.

The solubility parameter is commonly used to predict the solubility of one solid or liquid in another liquid. Similarly, the concept can be also introduced to predict the dissolution of hydrophobic UVA in a solid solvent such as PET, namely, exhaustion of UVA on PET. It was found that the hydrophobic small molecules with high sorption on PET tend to have solubility parameters near that of PET, δ 23.5 (J/cm³)^{0.5}. The solubility parameters of **CBHDCP**, **CBMPP** and Tinuvin 326 have been estimated using the group contribution method according to Eq. (1). Table 3 shows the solubility parameters of **CBHDCP**, **CBMPP**, Tinuvin 326 and PET. It is clearly presented in Tables 2 and 3 that the solubility parameters decrease in the order of **CBHDCP** > **CBMPP** > Tinuvin 326 > PET, and the exhaustion on PET increase in the order of **CBHDCP** < **CBMPP** < Tinuvin 326. The result agrees with previous studies that disperse dyes with high exhaustion on fiber have solubility parameters close to that of polymer.

5. Conclusions

Two highly efficient benzotriazole absorbers **CBHDCP** and **CBMPP** with single sharp absorption in a narrow range of 300–360 nm as well as strong absorption ability were successfully synthesized, and their structures were confirmed by FT-IR, ¹H NMR, mass spectroscopy, elemental analysis and quantum chemistry calculations. Systematic quantum chemistry calculations were performed to investigate the UV electronic absorption bands of

CBHDCP and **CBMPP** and found out the excellent absorption of **CBHDCP** and **CBMPP** come from $S_0 \rightarrow S_1$ electronic transition band of the Enol structures. To **CBHDCP-Enol**, the hydrogen bond interaction and solvent polar effect should be considered to simulate the UV absorption spectrum for its cyclic ketone structure. It was clear that the dyed fabrics by **CBHDCP** and **CBMPP** provided effective protection against UVR. Furthermore, the analysis about the solubility parameter of **CBHDCP** and **CBMPP** gave reasonable explanation for the exhaustion's difference for the two UVAs on PET fabrics. This work appears that cowork of quantum chemistry calculations and organic synthesis is very powerful to develop highly effective UV absorbers.

Acknowledgments

This work was supported by Zhejiang Provincial Key Innovation Team (No. 2010R50038), the National Natural Science Foundation of China (Nos. 21106135 and 51173168) and "521" talent cultivation of Zhejiang Sci-Tech University.

References

- [1] R.R. Cordero, P. Roth, A. Georgiev, *Energy Convers. Manage.* 46 (2005) 2907–2918.
- [2] D. Rosu, L. Rosu, C.N. Cascaval, *J. Photochem. Photobiol. A: Chem.* 194 (2008) 275–282.
- [3] N. Gandra, A.T. Frank, O.L. Gendre, *Tetrahedron* 62 (2006) 10771–10776.
- [4] K. Pei, Z. Cui, W. Chen, *J. Mol. Struct.* 1032 (2013) 100–104.
- [5] M. Zayat, P. Garaia-Parejo, D. Levy, *Chem. Soc. Rev.* 36 (2007) 1270–1281.
- [6] F. Waiblinger, J. Keck, M. Stein, *J. Phys. Chem. A* 104 (2000) 1100–1106.
- [7] J. Pospisil, S. Nespurek, *Prog. Polym. Sci.* 25 (2000) 1261–1335.
- [8] C. Wang, G. Qi, Y. Lin, *Sci. Technol.* 25 (1999) 167–169.
- [9] N.A. Evans, J. Rosevear, P.J. Waters, *Polym. Degrad. Stab.* 14 (1986) 263–384.
- [10] M.J. Frisch, G.W. Trucks, H.B. Schlegel, G.E. Scuseria, M.A. Robb, J.R. Cheeseman, Jr., J.A. Montgomery, T. Vreven, K.N. Kudin, J.C. Burant, J.M. Millam, S.S. Iyengar, J. Tomasi, V. Barone, B. Mennucci, M. Cossi, G. Scalmani, N. Rega, G.A. Petersson, H. Nakatsuji, M. Hada, M. Ehara, K. Toyota, R. Fukuda, J. Hasegawa, M. Ishida, T. Nakajima, Y. Honda, O. Kitao, H. Nakai, M. Klene, X. Li, J. E. Knox, H.P. Hratchian, J.B. Cross, C. Adamo, J. Jaramillo, R. Gomperts, R.E. Stratmann, O. Yazyev, A.J. Austin, R. Cammi, C. Pomelli, J.W. Ochterski, P.Y. Ayala, K. Morokuma, G.A. Voth, P. Salvador, J.J. Dannenberg, V.G. Zakrzewski, S. Dapprich, A.D. Daniels, M.C. Strain, O. Farkas, D.K. Malick, A.D. Rabuck, K. Raghavachari, J.B. Foresman, J.V. Ortiz, Q. Cui, A.G. Baboul, S. Clifford, J. Cioslowski, B.B. Stefanov, G. Liu, A. Liashenko, P. Piskorz, I. Komaromi, R.L. Martin, D.J. Fox, T. Keith, M.A. Al-Laham, C.Y. Peng, A. Nanayakkara, M. Challacombe, P.M.W. Gill, B. Johnson, W. Chen, M.W. Wong, C. Gonzalez, J.A. Pople, *Gaussian09, Rev. A 11*, Gaussian Inc., Pittsburgh, PA, 2009.
- [11] R.F. Fedors, *Polym. Eng. Sci.* 14 (1974) 147–154.
- [12] A.I. Vogel, B.S. Furniss, *Vogel's Textbook of Practical Organic Chemistry*, 4th ed., Longman, London, 1978.
- [13] J.B. Foresman, A. Frisch, *Exploring Chemistry with Electronic Structure Methods*, third ed., Gaussian Inc., Pittsburgh, PA, 2009.
- [14] K.M. Pei, F.L. Li, X.M. Zheng, *J. Raman Spectrosc.* 42 (2011) 1034–1038.
- [15] K.M. Pei, Y.F. Ma, X.M. Zheng, *J. Chem. Phys.* 128 (2008) 224310.